

**MOONQUAKE TRIGGERED MASS WASTING ON ICY WORLDS.** Mackenzie Mills<sup>1,2</sup>, Robert T. Pappalardo<sup>2</sup>, and Mark P. Panning<sup>2</sup>, <sup>1</sup>Johns Hopkins University, ([mmills23@jhu.edu](mailto:mmills23@jhu.edu)); <sup>2</sup>Jet Propulsion Laboratory, California Institute of Technology, ([pappalardo@jpl.caltech.edu](mailto:pappalardo@jpl.caltech.edu)), ([mark.p.panning@jpl.caltech.edu](mailto:mark.p.panning@jpl.caltech.edu)).

**Introduction:** High-resolution images of icy satellites, notably Ganymede and Enceladus, show a preponderance of tectonically deformed terrains, with little direct evidence for plains-style cryovolcanic resurfacing [1,2]. Regions smooth at global (1 km) and regional (100 m) imaging resolutions are generally found to be tectonically deformed at high (10 m) resolutions, with associated low-lying smooth materials between tectonic blocks. It is unclear whether tectonism alone can resurface terrains, or whether plains-style icy volcanism accompanies tectonism but is so intimately associated with tectonism that direct evidence for it is erased [1].

Mass wasting—the movement of eroded materials downslope—could potentially form smooth materials that cover local topographic lows, yet image resolution limitations necessarily limit the ability to study this process on icy satellites [3]. Here we investigate whether mass wasting can be triggered by tectonic activity on icy satellites. If so, we can further consider whether tectonically triggered mass wasting a feasible explanation for smooth material between inferred fault blocks.

We analyze *Galileo* images of Ganymede and *Cassini* images of Enceladus to infer fault dimensions and estimate seismic moments and moment magnitudes. We then infer seismic moments and moment magnitudes and consider feasible vertical ground accelerations based on numerical wave propagations. This permits us to infer whether these seismic events could trigger mass-wasting to account for smooth valley fill material.

**Procedure:** Seismic moment ( $M_o$ ) and moment magnitude ( $M_w$ ) are calculated using the equations:  $M_w = \frac{2}{3} \log M_o - 6.06$ ,  $M_o = \mu A d$  where  $\mu$  is the shear modulus for ice (here adopted as 3.521 GPa [5]) and  $M_o$  is in Nm. We measure fault length ( $L$ ), infer fault dip ( $\theta$ ) and dip-slope ( $W$ ), and then estimate fault full width ( $F$ ) to the brittle-ductile transition of  $2 \pm 1$  km [1] by modeling the brittle-ductile transition and calculating dips from image measurements. Using these parameters, we calculate fault area ( $A = L \cdot F$ ) and slip for an individual seismic event ( $d$ ) by assuming a self-similar scaling ratio with  $L$  of  $d/L = 10^{-5}$  [5–8], and also assuming scarps are generated from multiple slip events.

Fault dimensions are corrected for spacecraft viewing geometries—vertically from the emission angle ( $e$ ), and horizontally from the north azimuth angle ( $n$ ). Apparent scarp width ( $W'$ ), is maximized when  $|e|$  is small and when viewing toward the up-dip direction.

**Results:** We infer seismic moments of  $3 \times 10^{16}$  –  $5 \times 10^{18}$  Nm and moment magnitudes of 4.9 – 6.7 (Figure

1). On Europa, Nimmo and Schenk [6] modeled an observed scarp to produce events with a seismic moment of  $10^{17}$  Nm ( $M_w = 5.3$ ), based on an assumed 600 m slip event and  $\mu = 0.4$  GPa, assuming fractured ice, a value comparable with our calculated moment range for possible large events along observed fault scarps on Ganymede and Enceladus. No age or frequency is known for such seismic episodes, but observed total fault offsets suggest repeated events occurred along these fault lines. It is, however, important to note that the low gravity of these satellites compared to Earth may affect the size and frequency of seismic events, particularly through our assumed displacement to fault length scaling, because less force would be required to overcome the frictional resistance of near-surface ice.

Our calculated dips show peaks near  $25^\circ$  and  $45^\circ$ , with an average of  $33^\circ$ . A dip range  $45^\circ$  –  $60^\circ$  [10] fits about half our values, so some of the derived dips appear shallow for normal faults, which are expected to have dips near  $60^\circ$ . Such shallow dips may themselves be indicative of mass wasting, consistent with the notion of displaced material creating valley fill.

The resulting vertical seismic accelerations range from  $0.0047$  –  $8.0$  m/s<sup>2</sup> (Figure 2). We use an attenuation curve based on numerical wave propagations through a model of Ganymede [11] using numerical wave propagation simulations [12] estimated with the tools AxISEM [13] and Instaseis [14]. We derive peak ground accelerations that are comparable to the surface gravitational acceleration of Ganymede, within 10s to 100s km of the largest modeled events.

Given the magnitudes of estimated moonquakes and the resulting vertical accelerations, we conclude that seismic activity is a feasible process for generating mass wasting and smooth topography on icy satellites.

**References:** [1] Pappalardo et al. (2004), in *Jupiter* (F. Bagenal et al., eds.), 363. [2] Patterson et al. (2018) in *Enceladus and the Icy Moons of Saturn* (P. M. Schenk et al., eds.), 95. [3] Moore et al. (1999), *Icarus* 140, 294. [4] Pegler and Das (1996), *GRL* 23, 905–908. [5] Gudmundsson et al. (2013), *J. Struct. Geol.* 608, 1298. [6] Manighetti et al. (2005), *JGR* 110(B5). [7] Nicol et al. (2005), *J. Struct. Geol.* 27(2), 327. [8] Schultz et al. (2006), *J. Struct. Geol.* 28, 2182. [9] Nimmo and Schenk (2006), *J. Struct. Geol.* 28, 2194. [10] Beddingfield et al. (2015), *JGR Planets* 120, 2053. [11] Vance et al. (2018), *JGR Planets* 123(1), 180. [12] Stähler et al. (2018), *JGR Planets* 123, 206. [13] Nissen-Meyer et al. (2014), *Solid Earth* 425. [14] van Driel et al. (2015), *Solid Earth* 6, 701.

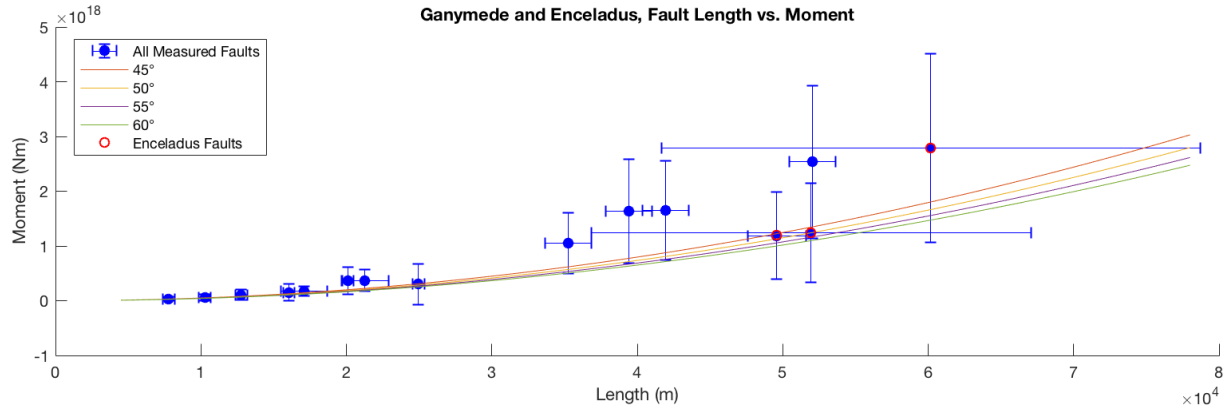


**Figure 1:** Calculated seismic moments for faults on Ganymede and Enceladus, as a function of fault length and dip. Uncertainties are propagated from image resolutions, with lower resolutions having a higher uncertainty resulting from stereo smoothing of topography.

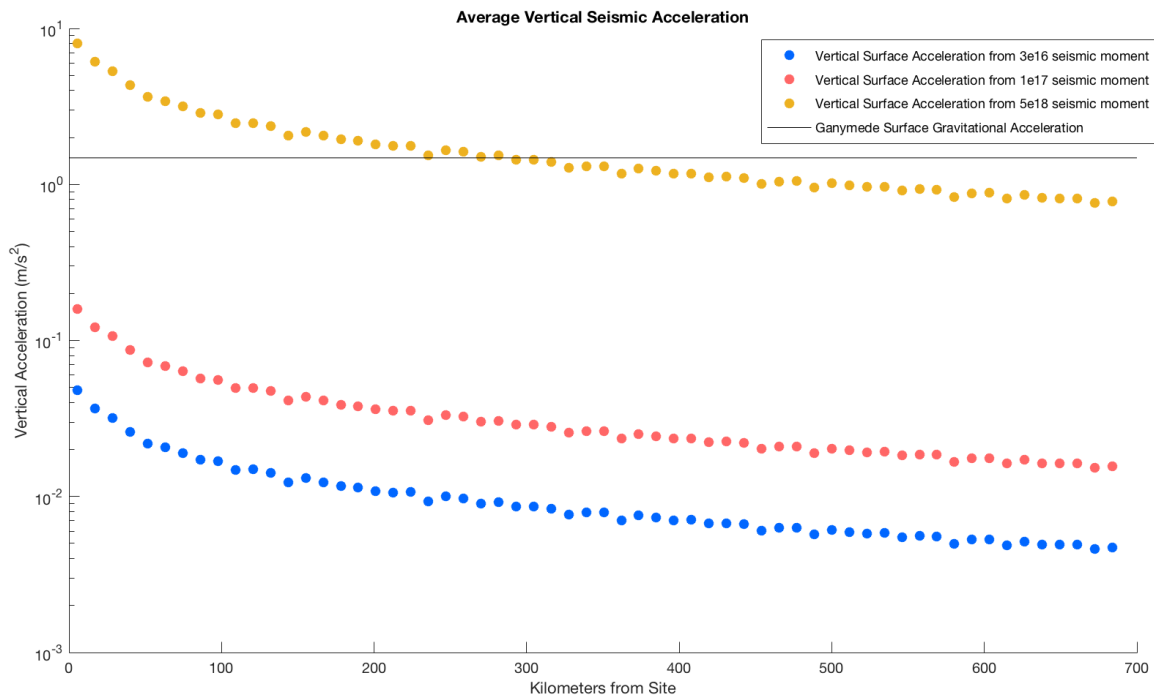


**Figure 2:** Modeled average vertical accelerations as a function of distance from the source, for three candidate events on Ganymede (yellow, red, and blue dots), compared with the surface gravitational acceleration (black line).